

An investigation of the submillimeter background radiation using SCUBA and Spitzer

S. Dye¹, S. A. Eales¹, M. L. N. Ashby², J. -S. Huang², T. M. A. Webb³, P. Barmby², S. Lilly⁴, M. Brodwin⁵, H. McCracken⁶, E. Egami⁷, G. G. Fazio²

ABSTRACT

We investigate the redshift dependence of the contribution to the extragalactic far-infrared/sub-millimeter background from galaxies detected by the Spitzer Space Telescope at $8\mu\text{m}$ and $24\mu\text{m}$. Using seven-band optical to mid-infrared photometry, we estimate photometric redshifts for the Spitzer sources which appear to be mostly L_* galaxies at a median redshift of $z = 1.0$. These sources, extracted from deep $8\mu\text{m}$ and $24\mu\text{m}$ mosaics of the CUDSS 14-hour field with 5σ limits of $5.8\mu\text{Jy}$ and $70\mu\text{Jy}$ respectively, exhibit significant $850\mu\text{m}$ and $450\mu\text{m}$ emission as observed by SCUBA. At $850\mu\text{m}$, after removing $\geq 4\sigma$ sources and those securely identified in our previous cross-matching paper, we measure stacked flux at the significance level of 4.4σ and 2.9σ from the full $8\mu\text{m}$ and $24\mu\text{m}$ galaxy catalogue respectively. At $450\mu\text{m}$, flux is detected from all $8\mu\text{m}$ galaxies at the level of 3.5σ , while there is no significant emission from the $24\mu\text{m}$ galaxies. We find that the $850\mu\text{m}$ flux is emitted almost exclusively at $z \gtrsim 1.3$ from the Spitzer sources with 0.44mJy (4.7σ) per $8\mu\text{m}$ source and 0.51mJy (2.8σ) per $24\mu\text{m}$ source. This corresponds to a contribution of $(16 \pm 3)\%$ toward the $850\mu\text{m}$ extra-galactic background from the $8\mu\text{m}$ sources and $(5.0 \pm 1.8)\%$ from the $24\mu\text{m}$ sources. At $450\mu\text{m}$, only the $8\mu\text{m}$ sources within the redshift interval $1 < z < 2$ exhibit significant emission with an average flux per source of 3.35mJy (3.0σ). This is a contribution of $(37 \pm 12)\%$ to the $450\mu\text{m}$ background.

Subject headings: infrared: galaxies

1. Introduction

Steady advances toward a thorough understanding of the population of high redshift sub-millimeter (submm) sources uncovered by the

Sub-millimeter Common User Bolometric Array (SCUBA) and the Max-Planck Millimeter Bolometer (MAMBO) have been made since their detection in the first deep submm survey by Smail, Ivison & Blain (1997). The two most controversial issues concerning their nature have been, firstly, identification of their dust-cloaked energy source and secondly, how they relate to local systems.

The question regarding the energy source has now been largely satisfied. The lack of strong X-ray emission from these sources (eg. Ivison et al. 2000b; Fabian et al. 2000; Alexander et al. 2003; Almaini et al. 2003; Waskett et al. 2003; Alexander et al. 2005) suggests that their submm flux is dominated by re-radiated emission from intense star formation, rather than AGN output. Observations constrain the net contribution of AGN activity to the level of $\sim 30\%$ (see Chapman et al.

¹School of Physics & Astronomy, Cardiff University, 5 The Parade, Cardiff, CF24 3YB, UK.

²Harvard Smithsonian Centre for Astrophysics, 60 Garden Street, Cambridge, MA 02138

³Sterrewacht Leiden, Neilss Bohrweg 2, Leiden 233CA, Netherlands

⁴Institute of Astronomy, Swiss Federal Institute of Technology Zurich, CH-8093 Zurich, Switzerland

⁵JPL, CalTech, M/S 169-506, 4800 Oak Grove Drive, Pasadena, CA 91109, USA

⁶Institute d'Astrophysique, 98bis, Bd Arago - 75014 Paris, France

⁷Steward Observatory, University of Arizona, 933 North Cherry Avenue, Tuscon, AZ 85721

2005, and references contained therein). However, the question regarding their relationship with the local galaxy population remains only partially answered.

Finding the connection between distant submm sources and local galaxies requires an understanding of their evolution. Sources detected in surveys with SCUBA and MAMBO have extremely high estimated star formation rates (100 - 1000 $M_{\odot} \text{ yr}^{-1}$), enough to rapidly form a massive elliptical (Smail, Ivison & Blain 1997; Hughes et al. 1998; Lilly et al. 1999; Dunne, Eales & Edmunds 2003). However, it is not clear from studies of the spatial density or clustering of submm sources whether a direct link between local ellipticals and the submm population can be made quite so confidently (Fox et al. 2002; Scott et al. 2002).

The main observational limitation in understanding the SCUBA population is the relatively large beam size. This gives rise to a correspondingly large uncertainty on extracted source positions and also means that confusion is a concern in deeper observations. One of the key ingredients needed to help resolve the evolutionary relationship between local and distant submm galaxies, determination of submm galaxy redshifts, is therefore especially difficult. A successful technique is to observe the sources using radio interferometry, as the surface density of radio sources is sufficiently low to make confident associations with coincident submm sources. The high astrometric precision in these radio data greatly eases the identification of optical counterparts for follow-up spectroscopy. Around two thirds of the submm sources detected at $850\mu\text{m}$ appear to have radio counterparts (eg. Ivison et al. 2002; Borys et al. 2004), but because the ratio of radio to submm flux decreases with increasing redshift (Carilli & Yun 1999), radio observations are biased toward lower redshift objects ($z \lesssim 3$). This method was recently applied by Chapman et al. (2005) using Keck spectroscopy to determine the redshifts of 73 submm sources cross-identified in VLA maps. They found a median redshift of $z \sim 2.2$.

A frequently ignored issue is that the sources in the bright SCUBA samples may not be representative of the extragalactic far-infrared/submm background radiation as a whole. Determining the nature of the individual sources that constitute the background is of the greatest importance be-

cause approximately 50% of the entire extragalactic background radiation (minus the CMB) is radiated in the submillimeter waveband (Fixsen et al. 1998). Yet the bright SCUBA sources for which there are redshifts may represent only a tiny fraction of this background. The problem is that the far-IR/submillimeter background is much brighter (~ 30 times greater in terms of νI_{ν}) where it peaks at $\sim 200\mu\text{m}$ than it is at $850\mu\text{m}$, the wavelength of the SCUBA surveys. At $850\mu\text{m}$, around 30% of the background can be resolved into sources brighter than 3mJy (eg. Hughes et al. 1998; Eales et al. 2000; Smail et al. 2002; Webb et al. 2003b; Chapman et al. 2005). Estimates of this fraction extend up to 60% for sources down to 1mJy (eg. Smail et al. 2002; Chapman et al. 2005). The sources for which Chapman et al. (2005) measured redshifts are radio-detected sources with $850\mu\text{m}$ fluxes brighter than $\simeq 3$ mJy. Using estimates of the spectral energy distributions of individual galaxies Chapman et al. (2005) concluded that their sample represents 30% of the background at $850\mu\text{m}$ but only about 2% of the background at $200\mu\text{m}$.

Therefore, despite the success of the work on the brighter SCUBA samples, there are many unanswered questions. For example, is the redshift distribution that Chapman et al. (2005) measure representative of the far-IR/submm background as a whole? Until the background at $200\mu\text{m}$ can be directly resolved into individual sources, the next best alternative is to study the SCUBA sources at fainter $850\mu\text{m}$ fluxes. Unfortunately, here one hits the obstacle of confusion.

There are two ways round this obstacle. One is to exploit gravitational lensing to mitigate the problem (eg. Smail et al. 2002). The second is the approach we adopt in this paper, using the SCUBA images to estimate the submillimeter fluxes of objects selected in other wavebands for which there are already accurate positions. Peacock et al. (2000) used this reverse procedure by stacking $850\mu\text{m}$ SCUBA detected emission from optical sources in the Hubble Deep Field North. This study identified significant submm emission from galaxies with high UV star formation rates. Serjeant et al. (2003) repeated this work replacing the optical data with $15\mu\text{m}$ ISO sources, but measured no emission. However, the much improved sensitivity and resolution of the Spitzer

Space Telescope (Werner et al. 2004) recently enabled Serjeant et al. (2004) to statistically detect $5.8\mu\text{m}$ and $8\mu\text{m}$ sources in $850\mu\text{m}$ and $450\mu\text{m}$ SCUBA data. Finally, Knudsen et al. (2005) recently detected significant $850\mu\text{m}$ emission from distant red galaxies selected by $J-K > 2.3$, finding that these sources are probably strong contributors to the far-IR/submm background.

In this paper, we stack $450\mu\text{m}$ and $850\mu\text{m}$ flux observed by SCUBA at the position of $8\mu\text{m}$ and $24\mu\text{m}$ Spitzer sources in the Canada-United Kingdom Deep Sub-millimeter Survey (CUDSS) 14-hour field. From these data, we estimate the fractional contribution from Spitzer sources to the extragalactic background at $850\mu\text{m}$ and $450\mu\text{m}$. Using a combination of ground-based optical, near infrared and Spitzer $3.6\mu\text{m}$ and $4.5\mu\text{m}$ observations, we compute photometric redshifts for the Spitzer sources, to investigate the epoch at which their attributed submm flux is emitted. This paper follows on from our previous paper (Ashby et al. 2005) where the forward approach of cross-identifying Spitzer sources with submm sources was carried out.

The layout of this paper is as follows: In Section 2 we describe the data. Section 3 details our photometric redshift estimation. Stacking is carried out in Section 4. We conclude with a summary and discussion in Section 5.

2. Data

Observations of the CUDSS 14 hour field analysed in this paper comprise three distinct sets: 1) Mid-infrared observations using the Spitzer Space Telescope, 2) Submm data observed with SCUBA, 3) Ground-based optical and near infrared observations.

2.1. Spitzer Space Telescope Data

The Spitzer observations discussed in this paper were obtained as part of the Guaranteed Time Observing program number 8 to image the extended Groth strip, a $2^\circ \times 10'$ area at $\alpha \sim 14^{\text{h}}19^{\text{m}}$, $\delta \sim 52^\circ 48'$ (J2000) with the Infra-red Array Camera (IRAC; Fazio et al. 2004) and Multi-band Imaging Photometer for Spitzer (MIPS; Rieke et al. 2004). Approximately 90% of the CUDSS 14 hour field falls robustly inside this area, the remaining 10% in the south-east corner having poor

or no coverage. This corner was cropped in all data sets presented here (see Figure 1).

Carrying on from our identification paper (Ashby et al. 2005), we have used the $8\mu\text{m}$ IRAC and $24\mu\text{m}$ MIPS source positions for the stacking. The fraction of sources detected in the higher frequency IRAC data that are dusty submm emitters is expected to be lower than in the $8\mu\text{m}$ and $24\mu\text{m}$ data. In addition, the sensitivity of these shorter wavelength data is much higher than the SCUBA maps so that the stacking tends to sample noise rather than the detectable population of faint sources. Indeed, Serjeant et al. (2004) failed to detect significant submm emission from Spitzer sources observed in the IRAC $3.6\mu\text{m}$ and $4.5\mu\text{m}$ channels in SCUBA observations of the Hubble Deep Field. The converse is true of the longer wavelength MIPS data where the number density of sources seen is too low to act as a good probe of the submm emission observed in our SCUBA maps. The 5σ point source sensitivity of the $8\mu\text{m}$ and $24\mu\text{m}$ data is $5.8\mu\text{Jy}$ and $70\mu\text{Jy}$ respectively.

Although we made no use of the $3.6\mu\text{m}$ and $4.5\mu\text{m}$ IRAC detected sources in the stacking directly, photometry from these channels was combined with the ground-based optical data for computation of photometric redshifts in Section 3. The 5σ point source sensitivity of both the $3.6\mu\text{m}$ and $4.5\mu\text{m}$ data is $0.9\mu\text{Jy}$.

There are 553 $8\mu\text{m}$ sources that fall within the $850\mu\text{m}$ map area and 511 that fall within the $450\mu\text{m}$ map. Of the $24\mu\text{m}$ sources, 141 fall within the $850\mu\text{m}$ map and 133 within the $450\mu\text{m}$ map. All of the $24\mu\text{m}$ sources are detected at $8\mu\text{m}$.

2.2. Sub-mm data

The SCUBA observations amount to 63 hours worth of data taken on 20 different nights over the period from March 1998 to May 1999 at the James Clark Maxwell Telescope (JCMT). The final $450\mu\text{m}$ and $850\mu\text{m}$ maps of the $\sim 7' \times 6'$ survey region were created by combining many 'survey units'. Each survey unit was observed for approximately one hour with a 64-point jiggle pattern (ensuring they are fully sampled), nodding JCMT's secondary mirror and chopping by $30''$ in right ascension.

The data reduction was carried out with the SURF package (Jenness 1997) and a noise map

created using a Monte Carlo technique to simulate the noise properties of each of SCUBA’s bolometers. We refer the reader to Eales et al. (2000) for more specific details of the data reduction.

We work with beam-convolved signal-to-noise (S/N) maps in this paper, to maximise source detection. Since the goal is to detect faint SCUBA sources buried in the map noise, prior to convolving with the beam, we subtracted SCUBA sources based on their submm S/N and their identifications in our previous paper (Ashby et al. 2005). For the $850\mu\text{m}$ data, we made three maps with different combinations of SCUBA sources removed to assess whether the stacking is influenced by this removal process. These three combinations are: 1) Removal of only the sources listed in Ashby et al. (2005) with a secure Spitzer identification. A ‘secure’ source is defined as having a bright $8\mu\text{m}$ positionally coincident ($r < 10''$) Spitzer counterpart with IRAC-MIPS colors indicative of a high-redshift dusty source (see Huang et al. 2004). Ashby et al. (2005) made 7 secure identifications. 2) Removal of the secure sources along with the remaining 5 sources detected by SCUBA with significance $\geq 4\sigma$. 3) Removal of the 12 sources in case 2 along with the remaining 6 sources having a ‘possible’ Spitzer identification at $8\mu\text{m}$. A source identification is classified as ‘possible’ when selected from multiple co-incident sources. As in case 1, the most likely counterpart is chosen based on IRAC-MIPS colors. Removing this last combination of 18 sources leaves only 2 of the 23 SCUBA sources in the $850\mu\text{m}$ data (three fall in the cropped south-eastern corner), both with significances of 3.0σ (Webb et al. 2003a).

Sources were removed from the raw SCUBA maps by subtracting the beam profile at the position of the source, scaled by the source flux. There are no directly detectable significant sources in the $450\mu\text{m}$ data, hence no sources were removed from the $450\mu\text{m}$ map. Figure 1 shows the beam-convolved S/N map at $850\mu\text{m}$ with the secure $+ \geq 4\sigma$ sources removed and the (unmodified) map at $450\mu\text{m}$. The $8\mu\text{m}$ and $24\mu\text{m}$ Spitzer source positions within the CUDSS 14h area having $z > 1.3$ are over-plotted on the $850\mu\text{m}$ map and those with $1 < z < 2$ are over-plotted on the $450\mu\text{m}$ map, to coincide with the findings of Section 4.2.

2.3. Optical & Near Infrared Data

In addition to the IRAC matched photometry, we also matched to optical and near-infrared ground-based data. For the optical photometry, we extracted U, B, V & I fluxes from the Canada-France Deep Fields survey (CFDF) (McCracken et al. 2001) imaged with the 4.0m Blanco Telescope and the Canada-France-Hawaii Telescope (CFHT). Like the IRAC photometry, fluxes were summed in $3''$ diameter apertures. The 3σ point source sensitivities in AB mags are 27.71, 26.23, 25.98 and 25.16 for U, B, V & I respectively.

For the near-infrared photometry, we matched to our own SExtracted (Bertin & Arnouts 1996) catalogue of the K-band image of Webb et al. (2003a), observed with the CFHT using the CFHTIR camera. The K-band data reach a depth of $K_{\text{AB}} \sim 23$.

3. Photometric Redshifts

From the matched aperture photometry in U, B, V, I & K as well as the IRAC $3.6\mu\text{m}$ and $4.5\mu\text{m}$ channels, we obtained photometric redshifts for the $8\mu\text{m}$ and $24\mu\text{m}$ sources using the HyperZ redshift code (Bolzonella et al. 2000). We decided not to use photometry from the two longest-wavelength IRAC channels, $5.8\mu\text{m}$ & $8\mu\text{m}$, because these data are less sensitive than the two shortest-wavelength channels, they are more affected by dust emission features (Lu et al. 2003) and the spectral templates are uncertain at these wavelengths (specifically, the contribution from PAHs). We excluded sources with poor quality measurements at $3.6\mu\text{m}$ and $4.5\mu\text{m}$, although we did not exclude sources with poor measurements or non-detections in the longer wavelength bands.

The local galaxy spectral energy distributions (SEDs) packaged with HyperZ are those given by Coleman et al. (1980), with an extrapolation into the infrared using the results of spectral synthesis models. The lack of any empirical basis for these templates at wavelengths $> 1\mu\text{m}$ is clearly unsatisfactory since our photometry includes both near-infrared and mid-infrared measurements. Therefore, we constructed our own set of templates in the following way. Mannucci et al. (2001) list empirical SEDs extended from $0.1\mu\text{m}$ to $2.4\mu\text{m}$ for the Hubble types E, S0, Sa, Sb and Sc. We extended these out to $6\mu\text{m}$ using the average SEDs

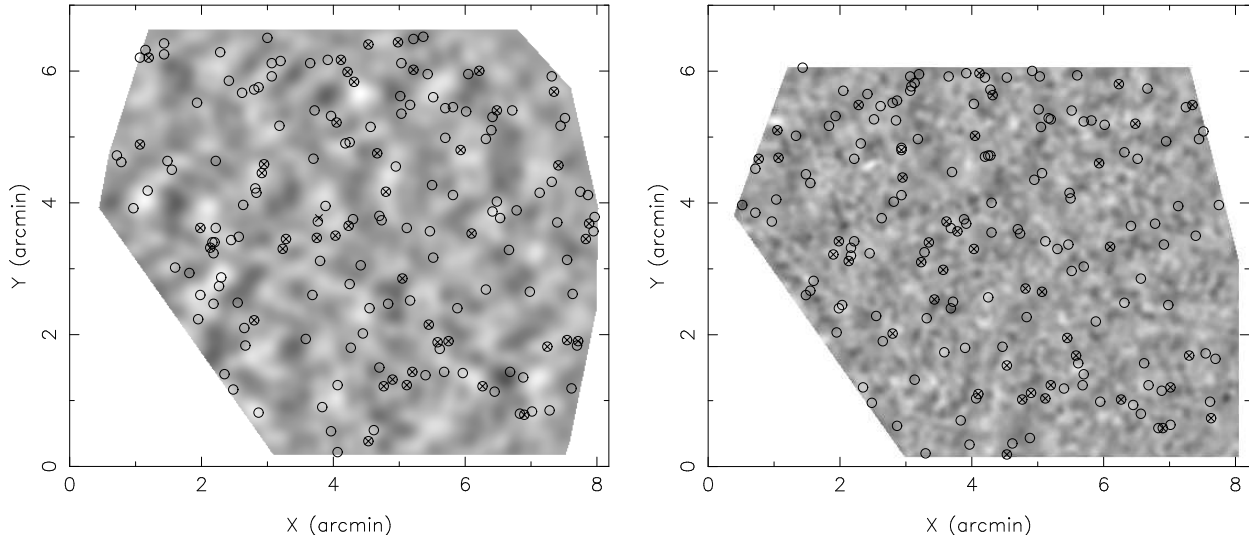


Fig. 1.— The CUDSS 14 hour field showing IRAC $8\mu\text{m}$ sources (circles) and MIPS $24\mu\text{m}$ sources (crosses) overlaid on the SCUBA data. *Left:* The $850\mu\text{m}$ beam-convolved map with $z > 1.3$ Spitzer sources overlaid (lighter shading indicates a higher submm flux). In this map, the ‘secure’ and $\geq 4\sigma$ SCUBA sources have been removed (see text). *Right:* The $450\mu\text{m}$ beam-convolved map with $1 < z < 2$ Spitzer sources overlaid. In both maps, the south-eastern (bottom-left) corner is cropped where there is no Spitzer coverage.

for disk galaxies and elliptical galaxies listed in Table 3 of Lu et al. (2003) using the disk-galaxy SED for all Hubble types apart from ellipticals. The one disadvantage of these templates is the lack of a template for an irregular galaxy, and we therefore retained the HyperZ template for an Im galaxy, extending this into the mid-infrared using the average disk-galaxy SED from Lu et al. (2003).

We tested the accuracy of our photometric redshifts by estimating redshifts for the $8\mu\text{m}$ sources in the field that have spectroscopically confirmed redshifts. There are 61 galaxies from the Canada-France Redshift Survey (CFRS) (Lilly et al. 1995) that are detected by Spitzer at $8\mu\text{m}$ and an additional four objects that are possible SCUBA detections with spectroscopic redshifts (Chapman et al. 2005). Figure 2 shows the photometric redshift estimates plotted against the spectroscopic redshifts. The agreement is fairly good with the scatter, defined as $\sqrt{\Sigma[\Delta z/(1+z)]^2/N}$, equal to 0.217 for the CFRS sources and 0.161 for the four SCUBA galaxies. We note, however, that there are very few galaxies with spectroscopic redshifts

at $z > 1$. We are therefore less confident about the accuracy of estimates beyond this redshift, although the large bin size used when stacking by redshift in Section 4.2 will greatly reduce the impact of large errors.

Figure 3 shows the I-band magnitude versus photometric redshift for all the objects in our $8\mu\text{m}$ and $24\mu\text{m}$ catalogue. The curve shows the prediction for a non-evolving L_* galaxy, with the K-correction calculated using the SED for an Sbc galaxy. We have used the value for L_* given by Blanton et al. (2001). The diagram shows that the galaxies detected by Spitzer at $8\mu\text{m}$ are mostly L_* galaxies with a fairly small dispersion about this luminosity. This small dispersion is additional confirmation that our photometric-redshift technique works reasonably well (approximately 50% more scatter is seen if the Spitzer photometry is omitted in the redshift analysis).

4. Stacking analysis

The stacking process determines the sum of the submm flux detected at the position of Spitzer

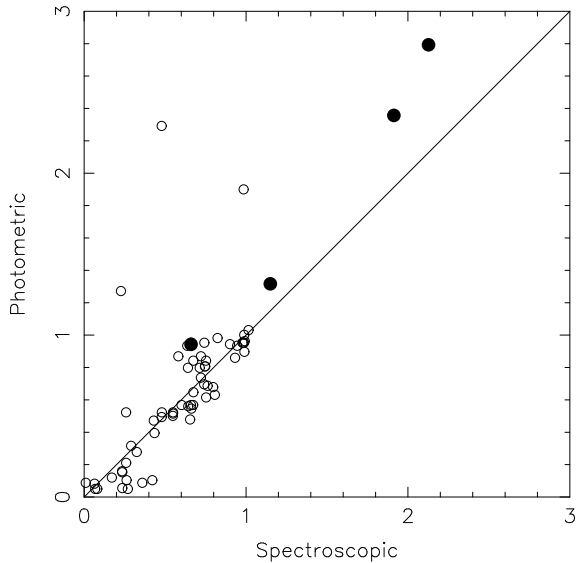


Fig. 2.— Comparison of photometric redshifts (using U, B, V, I, K, $3.6\mu\text{m}$ & $4.5\mu\text{m}$ fluxes) with spectroscopic redshifts for the $8\mu\text{m}$ sources in the CUDSS 14h field. Open circles show the 61 $8\mu\text{m}$ sources with redshifts measured by the CFRS. Filled circles are the 4 SCUBA sources with spectroscopic redshifts measured by Chapman et al. (2005).

sources and its significance. In this work, we calculate the total weighted flux, given by

$$f = N(\sum_i f_i \sigma_i^{-2}) / (\sum_i \sigma_i^{-2}), \quad (1)$$

where f_i is the submm flux taken from the beam-convolved map at the position of the i th Spitzer source, σ_i is its error and N is the total number of sources stacked.

We measure the significance of the stacking in two separate ways:

- The first uses the Kolmogorov-Smirnov (KS) test to quantify the significance of the discrepancy between the distribution of S/N drawn from the submm map at the position of the Spitzer sources and the S/N distribution of all pixels in the entire map. If the former distribution is positively skewed with respect to the latter, then this is attributed to the detection of faint SCUBA sources.
- The second is based on the significance of the actual total weighted flux measured. The

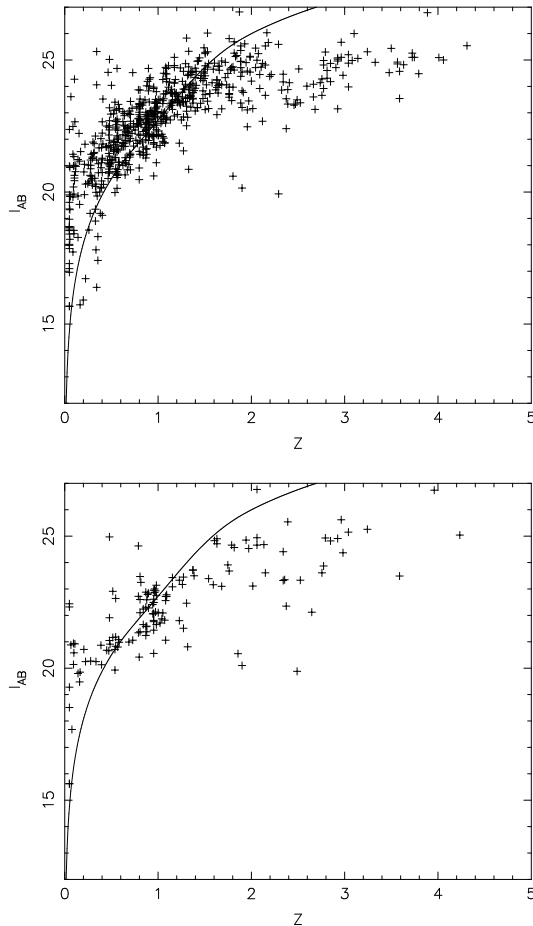


Fig. 3.— I-band magnitude versus photometric redshift for all $8\mu\text{m}$ sources (*top*) and $24\mu\text{m}$ sources (*bottom*). Solid line shows prediction for a non-evolving L_* Sbc galaxy.

formal error on f is defined as

$$\sigma_f = N / \sqrt{\sum_i \sigma_i^{-2}}. \quad (2)$$

One can then define the significance $\beta = f / \sigma_f$. However, Serjeant et al. (2003) showed using Monte Carlo simulations that β is not normally distributed. We correct for this with our own Monte Carlo simulations (see below).

We determined the distribution of β and the KS significance by carrying out Monte Carlo simulations for each of the four SCUBA datasets considered in this paper (the three $850\mu\text{m}$ maps and the

450 μm map). 100,000 realisations of the Spitzer source positions were performed per dataset. We found that the distribution of KS significance is perfectly Gaussian in every case, whereas the distribution of β is skewed positively by an amount depending on the submm dataset.

To account for the non-Gaussianity in β , we used its distribution function calculated from the Monte Carlo analysis to make plots showing the relationship between β and its equivalent Gaussian significance, β_g . All four SCUBA datasets gave linear relationships which were fitted as follows: 850 μm secure $\beta_g = 0.79\beta - 0.15$; 850 $\mu\text{m} \geq 4\sigma$ + secure $\beta_g = 0.95\beta - 0.09$; 850 μm possible + secure $\beta_g = 1.01\beta - 0.22$; 450 μm $\beta_g = 0.86\beta + 0.26$. From these relationships, it is apparent that the 850 μm data with only secure sources removed would quite heavily over-predict the stacking significance if not corrected. The corrections for the remaining SCUBA data are fairly modest.

In this paper, all total weighted flux significances quoted are the corrected version β_g . Absolute errors quoted on the total weighted flux are those given by equation (2).

Despite the fact that the KS significance adheres to Gaussian statistics, we found that it often gives false peaks in simulations of alignment maps described in the following section, whereas the corrected weighted flux significance, β_g , does not. For this reason, we use β_g to assess data alignment. However, in Section 4.2 where we discuss stacking Spitzer sources selected by redshift, we calculate both β_g and the KS significance for comparison.

4.1. Stacking the full 8 μm & 24 μm catalogues

A crucial assumption in the stacking analysis is that the astrometric solutions of the Spitzer and SCUBA datasets are not offset from each other. We therefore tested the alignment of the SCUBA and Spitzer data by calculating β_g for a range of offsets in RA and Dec added to the Spitzer source positions. The test plots this as a map with the x-axis corresponding to the RA offset and the y-axis the Dec offset. If the Spitzer data is well aligned with the SCUBA maps *and* if a significant detection is made, a peak in the vicinity of the origin should be apparent. This peak should be

singular. If more than one significant peak is seen, then the alignment of both data sets cannot be established with confidence and the robustness of the detection must also be drawn into question.

Figure 4 shows the maps of β_g over the 100'' range of offsets in RA and Dec spanned, for both 8 μm and 24 μm Spitzer sources stacked with the 450 μm data and the 850 μm data with secure + $\geq 4\sigma$ sources removed. The contours start at a significance of 2σ with intervals of 0.5σ . The more smoothly varying features of the 850 μm plots relative to the 450 μm plots reflects the larger beam size at 850 μm .

Stacking the 8 μm sources shows a clear detection at both 850 μm and 450 μm with peak significances of 4.4σ and 3.5σ respectively. The 850 μm peak occurs at an offset of $(0'', -2'')$ and the 450 μm peak at $(4'', 0'')$. The results from stacking with the 24 μm catalogue are less clear; at 850 μm , there are two 2.9σ peaks at offsets of $(5'', -10'')$ and $(-8'', 12'')$ with a significance of 2.5σ at $(0'', 0'')$. There is no detection of the 24 μm sources at 450 μm .

To determine the significance of these offsets, we carried out Monte Carlo simulations of the stacking at 850 μm and 450 μm . For each realisation, we created a noisy synthetic SCUBA map and placed sources with fixed S/N by adding the SCUBA beam at random positions. After convolving the map with the beam, stacking was carried out, offsetting this randomized catalogue by varying amounts to produce a β_g map, like those shown in Figure 4. We carried out 200 realisations for each of five different source S/N values.

Figure 5 shows the mean and scatter of the radial offset of the peak in β_g from $(0'', 0'')$ as a function of the significance of the peak. We found no discernible difference between the 850 μm and 450 μm results hence this plot serves for both wavelengths. From the plot, we conclude that the peak of 4.4σ seen in the significance map for the 8 μm sources and 850 μm data, occurs on average in the simulations at a radial offset of $r = 2.0'' \pm 1.5''$. The measured offset of $(0'', -2'')$ is therefore consistent with there actually being no misalignment between the 850 μm SCUBA map and 8 μm data. Similarly, at 450 μm , the offset of $(4'', 0)$ of the 3.5σ peak is consistent with the expected offset of $r = 2.6'' \pm 1.7''$ for no misalignment. The implication that the 450 μm and 850 μm maps are well-

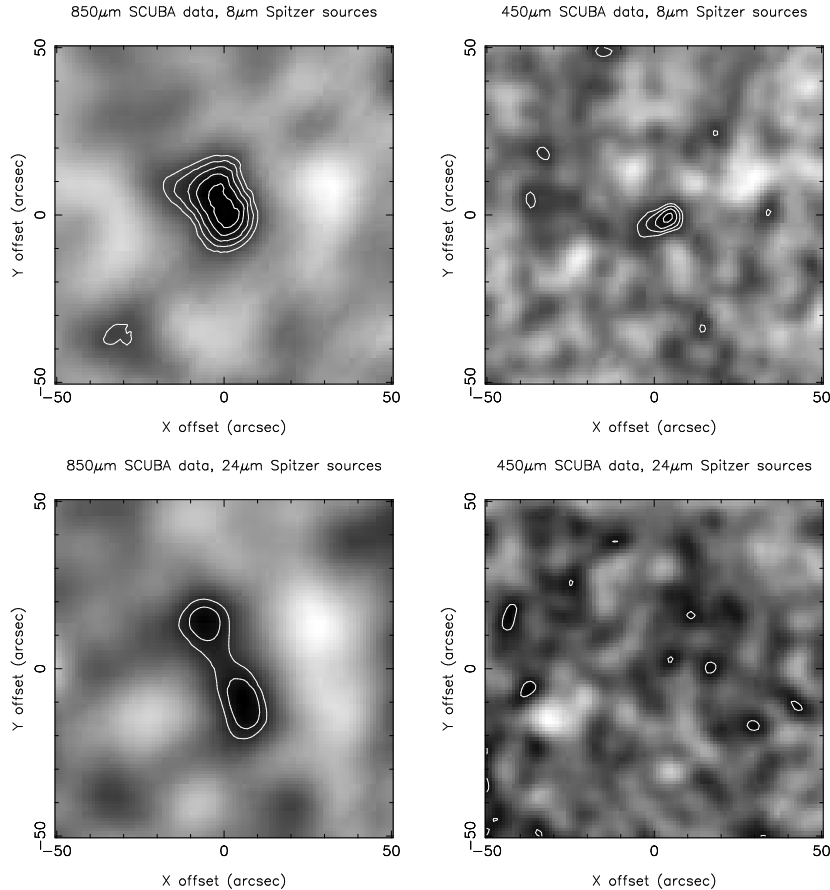


Fig. 4.— Variation of the total weighted submm flux significance, β_g , as a function of the offset of the SCUBA maps from the Spitzer source catalogue (i.e. add offset to Spitzer position to get SCUBA position). Contours start at 2σ level and have intervals of 0.5σ . Top row shows results for the $8\mu\text{m}$ Spitzer sources and the bottom row shows the $24\mu\text{m}$ source results. The $850\mu\text{m}$ map has secure $+ \geq 4\sigma$ submm sources removed; no submm sources are removed from the $450\mu\text{m}$ map.

aligned is reassuring; as an additional check, we verified that this is the case from astrometry of point source calibrators acquired at both wavelengths throughout the CUDSS observing. The $24\mu\text{m}$ catalogue has the same astrometry as the $8\mu\text{m}$ catalogue since both are tied to the Two Micron All Sky Survey (2MASS; Cutri et al. 2003), hence we conclude that all datasets used in the stacking are properly aligned.

To summarise this section, we can make two statements. Firstly, there is significant emission at $850\mu\text{m}$ and $450\mu\text{m}$ from all $8\mu\text{m}$ Spitzer sources on average. From the $24\mu\text{m}$ sources, the total weighted flux has a significance of 2.5σ at $850\mu\text{m}$ but because the significance map is dual-peaked,

this is a tentative detection. Secondly, the Spitzer data and the SCUBA data are well-aligned.

In the next section, we split the Spitzer catalogues by redshift to investigate the possibility of this detection being weakened by foreground/background Spitzer sources not truly associated with the observed submm emission.

4.2. Stacking by redshift

Having assigned photometric redshifts to the Spitzer catalogues, we can stack sources separated into redshift bins. The bin size must be large compared to the typical redshift uncertainty. In addition, the number of objects per bin must be

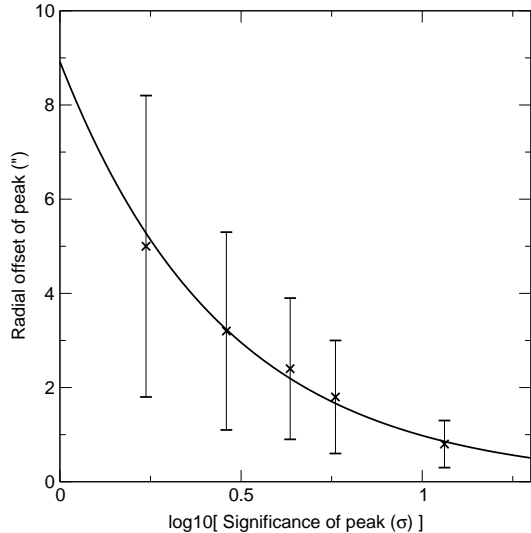


Fig. 5.— Results of Monte Carlo simulations to determine the variation of the mean and scatter of peak offset from ($0''$, $0''$) in the significance maps as a function of the amplitude of the peak measured. Results plotted here apply to the $8\mu\text{m}$ sources and either $850\mu\text{m}$ or $450\mu\text{m}$ data.

equal so that the significance across bins can be fairly compared (i.e. to keep Poisson noise constant per bin). Given the accuracy of our photometric redshifts discussed in Section 3, we split the $8\mu\text{m}$ sources into 6 redshift bins and the $24\mu\text{m}$ sources into 5. This gives an average bin width of $\Delta z \sim 0.5$. Stacking was then carried out for each bin at both $850\mu\text{m}$ and $450\mu\text{m}$.

The total weighted flux from all sources in a given redshift bin (expressed in units of MJy/sr) is plotted against the median bin redshift in Figure 6. The $850\mu\text{m}$ data show a clear detection with both $8\mu\text{m}$ and $24\mu\text{m}$ Spitzer sources lying at $z \gtrsim 1.3$. With the $450\mu\text{m}$ data, only the $8\mu\text{m}$ Spitzer sources produce a notable detection at $z \sim 1.5$.

Choosing our most conservative $850\mu\text{m}$ dataset, that with all secure and possible sources removed, and selecting Spitzer sources with $z > 1.3$, we found that the $8\mu\text{m}$ sources are detected at the level of 4.7σ and the $24\mu\text{m}$ sources at 2.8σ . At $450\mu\text{m}$, the $8\mu\text{m}$ sources selected by $1 < z < 2$ are detected with a significance of 3.0σ . The $24\mu\text{m}$ Spitzer sources selected by $1 < z < 2$ are not detected.

These detections were verified with the KS test. We applied the same Spitzer source redshift selections and chose the $850\mu\text{m}$ data with secure and possible sources removed. Figure 7 shows the results. In these plots, the S/N distribution of the full SCUBA map (the ‘map distribution’) is shown as an open histogram and the distribution of S/N at the redshift selected Spitzer source positions (the ‘source distribution’) as a shaded histogram. In all plots, bar that for the $450\mu\text{m} + 24\mu\text{m}$ data, excess emission from faint submm sources causes the source histogram to be clearly skewed positively with respect to the map histogram. The KS test quantifies the significances of these skews as follows: $850\mu\text{m}$ emission from the $8\mu\text{m}$ sources at 4.5σ , $850\mu\text{m}$ emission from the $24\mu\text{m}$ sources at 3.3σ and $450\mu\text{m}$ emission from the $8\mu\text{m}$ at 2.3σ . The $24\mu\text{m}$ sources are not detected at $450\mu\text{m}$.

Table 1 summarises the results for all versions of the submm data. The weighted flux significances agree fairly well with the KS significances, although on the whole, they are slightly higher. The largest discrepancy occurs in the $850\mu\text{m}$ map with only secure sources removed. In this case, the $\geq 4\sigma$ submm sources and/or the submm identifications defined as possible by Ashby et al. (2005) are detected in the stacking.

5. Summary and Discussion

We have measured significant $850\mu\text{m}$ emission from Spitzer $8\mu\text{m}$ and $24\mu\text{m}$ sources and $450\mu\text{m}$ emission from the $8\mu\text{m}$ sources. The 5σ point source sensitivities of the Spitzer data are 5.8mJy at $8\mu\text{m}$ and $70\mu\text{Jy}$ at $24\mu\text{m}$. By computing photometric redshifts for the Spitzer sources using optical, near infra-red and Spitzer $3.6\mu\text{m}$ and $4.5\mu\text{m}$ photometry, we have been able to statistically identify the epoch from which this submm emission dominates. We find that the $850\mu\text{m}$ flux is almost exclusively emitted from Spitzer sources at redshifts $z \gtrsim 1.3$ up to the highest redshift of $z \sim 4$ we measure in our sample. Our most conservative estimate of this flux (i.e. having subtracted secure and possible SCUBA sources) is 0.44mJy per $8\mu\text{m}$ Spitzer source (4.7σ significance) and 0.51mJy per $24\mu\text{m}$ Spitzer source (2.8σ significance). At $450\mu\text{m}$, the emission appears to peak around $z \sim 1.5$ with an average stacked flux per $8\mu\text{m}$ Spitzer source within $1 < z < 2$ of 3.35mJy

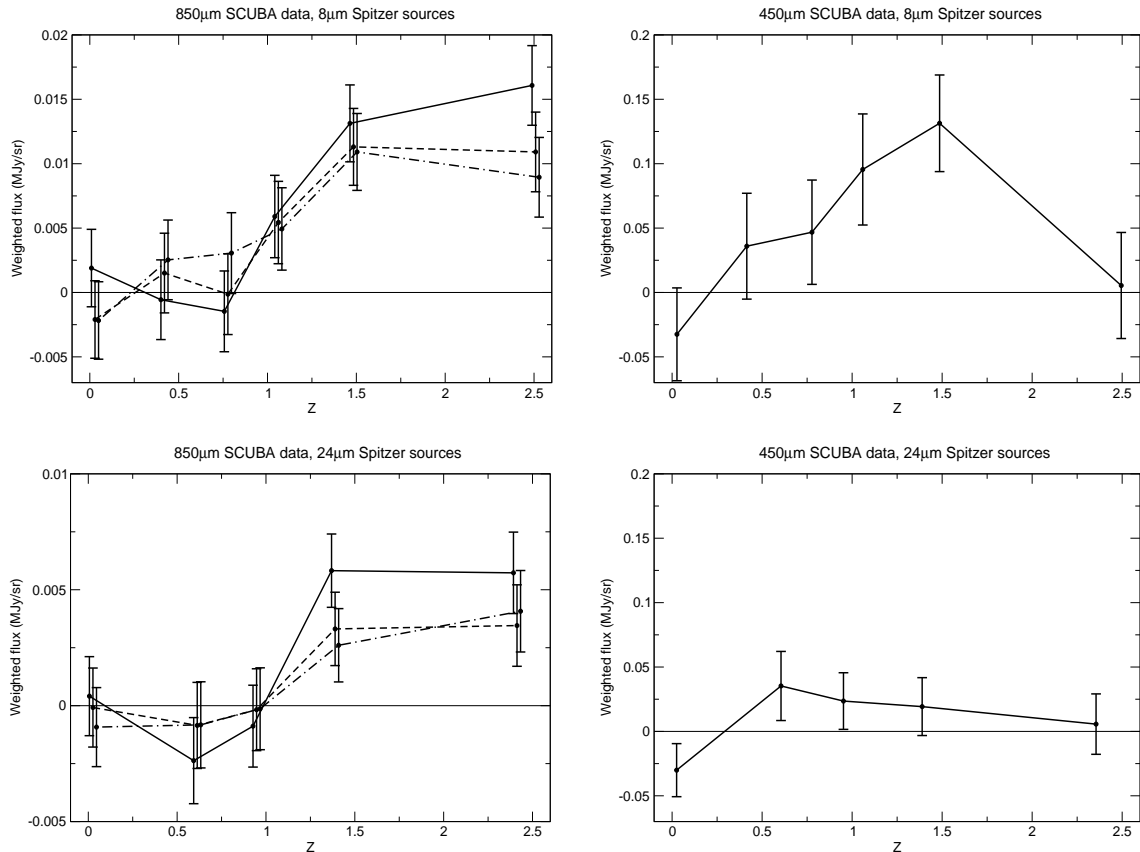


Fig. 6.— Variation of total weighted flux of objects binned by redshift (median bin redshift plotted). *Top left:* The $850\mu\text{m}$ data stacked with the $8\mu\text{m}$ sources, where the solid, dashed and dot-dashed lines indicate secure, secure + $\geq 4\sigma$ and secure + possible SCUBA source subtraction, respectively. Abscissae are plotted slightly staggered for clarity. *Top right:* The $450\mu\text{m}$ data stacked with the $8\mu\text{m}$ sources. *Bottom left:* $850\mu\text{m}$ data stacked with the $24\mu\text{m}$ sources. *Bottom right:* $450\mu\text{m}$ data stacked with the $24\mu\text{m}$ sources.

(3.0σ significance).

We can estimate the contribution our stacked flux makes to the extragalactic far-IR/submm background using the spectrum of Fixsen et al. (1998). According to their measurements, the background flux at $850\mu\text{m}$ is 0.14MJy/sr . The total weighted flux we measure from $8\mu\text{m}$ sources at $z > 1.3$ in our $850\mu\text{m}$ map with secure and possible sources removed is $0.022 \pm 0.004\text{MJy/sr}$, a contribution of $(16 \pm 3)\%$. The $24\mu\text{m}$ sources at $z > 1.3$ are responsible for approximately one third of this with a fractional contribution of $(5.0 \pm 1.8)\%$. At $450\mu\text{m}$, Fixsen et al. (1998) measure a background flux of 0.47MJy/sr . The weighted total flux from the $8\mu\text{m}$ sources with $1 < z < 2$ in our $450\mu\text{m}$ data is $0.175 \pm 0.058\text{MJy/sr}$, some

$(37 \pm 12)\%$ of the background.

Our estimate of the $850\mu\text{m}$ contribution to the background from $8\mu\text{m}$ sources is consistent with the fraction of $(20 \pm 8)\%$ determined by Serjeant et al. (2004). Within their errors, Serjeant et al. (2004) find that the $450\mu\text{m}$ flux from $8\mu\text{m}$ sources is sufficient to account for all of the background radiation at this wavelength. This is in contrast to our findings that indicate a maximum contribution of approximately 50%.

Including the flux of submm sources removed from the $850\mu\text{m}$ data gives a measure of the combined contribution of directly detected and stacked sources to the background at this wavelength. The secure and possible submm sources have a total weighted $850\mu\text{m}$ flux of $(62 \pm 5)\text{mJy}$. Adding this

SCUBA data	KS Significance		Submm flux (MJy/sr)	
	8 μ m sources	24 μ m sources	8 μ m sources	24 μ m sources
850 μ m – secure	4.8 σ	2.6 σ	0.032 \pm 0.004 (172, 5.5 σ)	0.011 \pm 0.002 (45, 3.9 σ)
850 μ m – (secure + $\geq 4\sigma$)	4.7 σ	3.4 σ	0.024 \pm 0.004 (172, 5.1 σ)	0.007 \pm 0.002 (45, 2.7 σ)
850 μ m – (secure + poss.)	4.5 σ	3.3 σ	0.022 \pm 0.004 (172, 4.7 σ)	0.007 \pm 0.002 (45, 2.8 σ)
450 μ m	2.3 σ	< 1 σ	0.175 \pm 0.056 (170, 3.0 σ)	0.035 \pm 0.027 (41, 1.4 σ)

Table 1: Spitzer 8 μ m and 24 μ m source detections at 850 μ m and 450 μ m. Redshift selection $z > 1.3$ applies to the 850 μ m data and $1 < z < 2$ applies to the 450 μ m data. Listed are the significances of the KS tests and the total weighted submm flux of all objects within the corresponding redshift selection. Quantities in brackets list the number of Spitzer galaxies stacked and the significance of the weighted flux, β_g (note that this is not the ratio flux/error due to its non-Gaussian distribution – see text).

to the stacked 850 μ m flux from the 8 μ m sources gives a total fractional background contribution of $(29 \pm 3)\%$. Webb et al. (2003c) estimate that Lyman break galaxies (LBGs) contribute $\sim (20 \pm 10)\%$ of the 850 μ m background. Even making the extreme assumption that there is absolutely no overlap between the LBG and Spitzer 8 μ m population (but see Huang et al. 2005, who estimate an overlap of $\sim 25\%$) the total fraction of the 850 μ m background that remains unaccounted for is at least 40%.

The average submm fluxes we measure in the stacking correspond to fairly regular systems. To demonstrate this, we can use the definition of an ultra-luminous infrared galaxy (ULIRG) set by Clements, Saunders & McMahon (1999). This stipulates that a ULIRG must have a luminosity of at least $10^{11.4}L_{\odot}$ measured at 60 μ m by the infra-red astronomical satellite (IRAS). With an assumed IRAS galaxy SED, the expected 850 μ m and 450 μ m flux can be calculated for a ULIRG at the median redshift of our catalogue, $z = 1.0$. Following Clements et al. (2004), we take the coolest and warmest IRAS galaxy SEDs from the sample of Dunne & Eales (2001) to estimate the range of submm emission expected. Using the SED of NGC958, which is dominated by cold dust at 20K, the expected submm flux from an object with a 60 μ m IRAS flux of $10^{11.4}L_{\odot}$ at $z = 1.0$ is 0.77mJy at 850 μ m and 2.06mJy at 450 μ m ($h_{100} = 0.7$, $\Omega_m = 0.3$, $\Lambda = 0.7$). Similarly, the SED of IR1525+36 has a much warmer mix of dust with temperatures 26K and 57K in the ratio 15:1, and predicts a flux of 0.06mJy at 850 μ m and 0.20mJy at 450 μ m. The average stacked 850 μ m and 450 μ m fluxes of 0.44mJy and 3.35mJy we measure from the 8 μ m Spitzer sources indicates that our stack-

ing is sensitive to borderline ULIRGS. Although ULIRGS would be considered extreme systems in the local universe, at $z \sim 1$, they are quite the norm (eg. Daddi et al. 2005).

An interesting result is the peak in 450 μ m emission we measure from the 8 μ m sources around $z = 1.5$. At this wavelength, the energy density of the background is approximately 25% of the maximum at $\sim 200\mu$ m (compared to only 3% at 850 μ m). Given that the 8 μ m sources make up a significant fraction of the 450 μ m background, it would not be unreasonable to expect that the entire far-IR/submm background is dominated by systems around this redshift. This is a slightly lower redshift than the median redshift $z = 2.2$ of the population of radio detected submm galaxies studied by Chapman et al. (2005). However, the Chapman et al. sample is substantially brighter (by $\times 40$) on average than the submm galaxies probed by the stacking in our work. This is consistent with the downsizing scenario in which larger galaxies generally form earlier than smaller galaxies. However, this result could be heavily influenced by difficult to quantify, varying selection effects between both studies. Clearly, we must wait for observations with a high 200 μ m sensitivity to provide a complete and definitive answer as to the nature of the far-IR/submm background.

Acknowledgements

This work is based on observations made with the Spitzer Space Telescope, which is operated by the Jet Propulsion Laboratory, California Institute of Technology under NASA contract 1407. Support for this work was provided by NASA through contract 1256790 issued by JPL/Caltech.

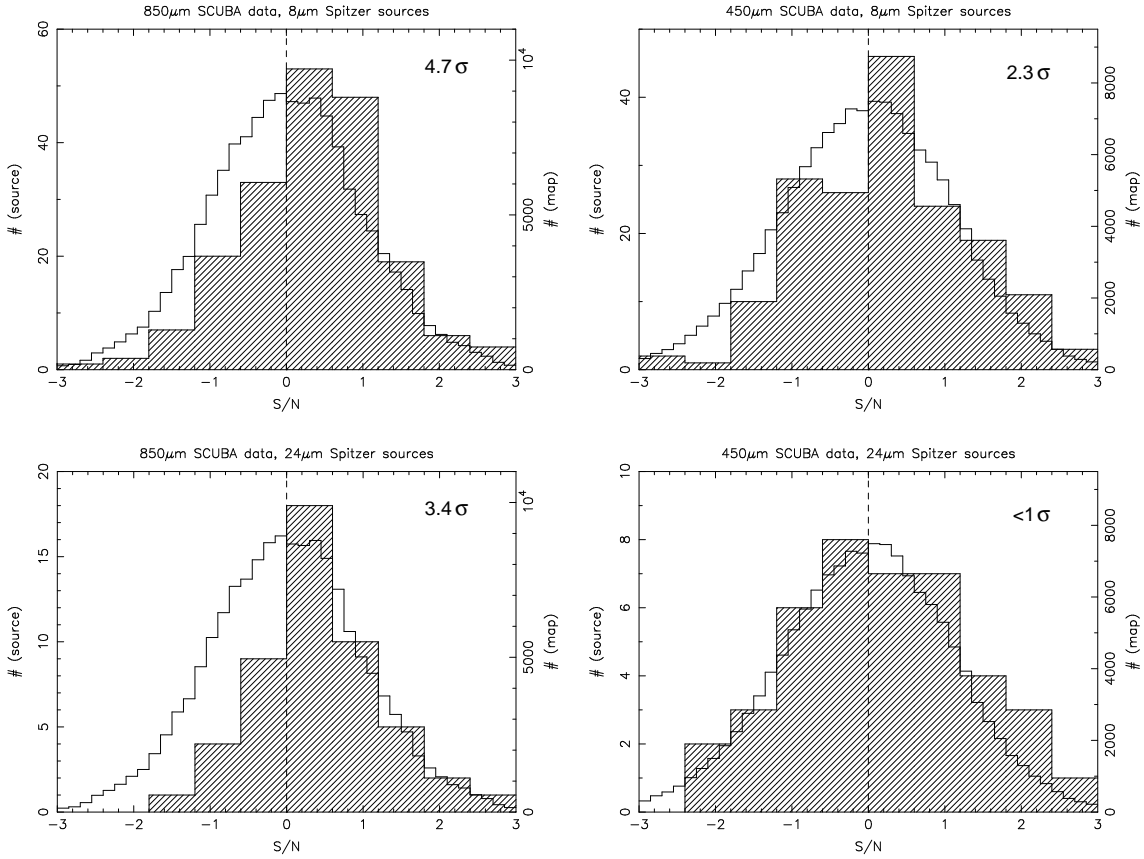


Fig. 7.— Distribution of submillimeter S/N at the positions of the Spitzer sources (*shaded histogram, left ordinates*) compared with the distribution of S/N over the entire SCUBA map (*open histogram, right ordinates*). For the $850\mu\text{m}$ data, secure $+ \geq 4\sigma$ SCUBA sources are removed and $z > 1.3$ Spitzer sources are selected. No SCUBA sources are removed from the $450\mu\text{m}$ data and $1 < z < 2$ Spitzer sources are selected.

REFERENCES

- Alexander, D.M., et al., 2003, *AJ*, 125, 383
- Alexander, D.M., Smail, I., Bauer, F.E., Chapman, S.C., Blain, A.W., Brandt, W.N., Ivison, R.J., 2005, *Nature*, 434, 738
- Almaini, O., et al., 2003, *MNRAS*, 338, 303
- Ashby, M.L.N., Huang, J.-S., Dye, S., Eales, S., Webb, T., Barmby, P., Rigopoulou, D., Egami, E., McCracken, H., Lilly, S., Miyazaki, S., Fazio, G.G., 2005, submitted to *ApJ*
- Bertin, E. & Arnouts, S., 1996, *A&AS*, 117, 393
- Blanton, M.R. et al., 2001, *AJ*, 121, 2358
- Borys, C., et al., 2004, *MNRAS*, 355, 485
- Bolzonella, M., Miralles, J.-M., Pelló, R., 2000, *A&A* 363, 476
- Carilli, C.L., & Yun, M., 1999, *ApJ*, 513, 13L
- Chapman, S.C., Blain, A.W., Smail, I., Ivison, R.J., 2005, *ApJ*, 622, 772
- Clements, D.L., Saunders, W.J. & McMahon, R.G., 1999, *MNRAS*, 302, 391
- Clements, D., et al., 2004, *MNRAS*, 351, 447
- Coleman, G.D., Wu, C.-C. & Weedman, D.W., 1980, *ApJS*, 43, 393
- Cutri, R.M., et al. 2003, Explanatory Supplement to the 2MASS Second Incremental Data Release, IPAC

- Daddi, E., et al., 2005, ApJ, 631, L13
- Dunne, L., & Eales, S.A., 2001, MNRAS, 327, 697
- Dunne, L., Eales, S.A. & Edmunds, M.G., 2003, MNRAS, 341, 589
- Eales, S., Lilly, S., Gear, W., Dunne, L., Bond, J. R., Hammer, F., Le Fèvre, O., Crampton, D., 1999, ApJ, 515, 518
- Eales, S., Lilly, S., Webb, T., Dunne, L., Gear, W., Clements, D., Yun, M., 2000, AJ, 120, 2244
- Fabian, A. C., Smail, Ian, Iwasawa, K., Allen, S. W., Blain, A. W., Crawford, C. S., Ettori, S., Ivison, R. J., Johnstone, R. M., Kneib, J.-P., Wilman, R. J., 2000, MNRAS, 315, 8
- Fazio, G.G., et al., 2004, ApJS, 154,10
- Fixsen, D.J., Dwek, E., Mather, J.C., Bennet, C.L., Shafer, R.A., 1998, ApJ, 508, 123
- Fox, M.J., et al., 2002, MNRAS, 331, 839
- Huang, J.-S., et al., 2004, ApJS, 154, 44
- Huang, J.-S., et al., 2005, ApJ in press, astro-ph/0507685
- Hughes, D.H., et al., 1998, Nat., 394, 241
- Ivison, R. J., Smail, Ian, Barger, A. J., Kneib, J.-P., Blain, A. W., Owen, F. N., Kerr, T. H., Cowie, L. L., 2000, MNRAS, 315, 209
- Ivison, R.J, et al., 2002, MNRAS, 337, 1
- Jenness, T., 1997, SURF-SCUBA User Reduction Facility, Starlink User Note 216.1
- Knudsen, K. K., van der Werf, P., Franx, M., Frster Schreiber, N. M., van Dokkum, P. G., Illingworth, G. D., Labb, I., Moorwood, A., Rix, H.-W., Rudnick, G., 2005, ApJ, 632, 9
- Lilly, S.J., Hammer, F., Le Fèvre, O., Crampton, D., 1995, ApJ, 455, 75
- Lilly, S.J., Eales, S.A., Gear, K.P., Hammer, F., Le Fèvre, O., Crampton, D., Bond, J.R., Dunne, L., 1999, ApJ, 518, 641
- Lu, N., Helou, G., Werner, M.W., Dinerstein, H.L., Dale, D.A., Silbermann, N.A., Malhotra, S., Beichman, C.A., Jarrett, T.H., 2003, ApJ, 588, 199
- Mannucci, E., Basile, F., Poggianti, B.M., Cimatti, A., Daddi, E., Pozzetti, L., Vanzi, L., 2001, MNRAS, 326, 745
- McCracken, H. J., Le Fèvre, O., Brodwin, M., Foucaud, S., Lilly, S. J., Crampton, D., Mellier, Y., 2001, A&A, 376, 756
- Peacock, J.A., et al., 2000, MNRAS, 318, 535
- Rieke, G., et al., 2004, ApJS, 154, 25
- Scott, S.E. et al., 2002, MNRAS, 331, 817
- Serjeant, S., Dunlop, J. S., Mann, R. G., Rowan-Robinson, M., Hughes, D., Efstathiou, A., Blain, A., Fox, M., Ivison, R. J., Jenness, T., Lawrence, A., Longair, M., Oliver, S., Peacock, J. A., 2003, MNRAS, 344, 887
- Serjeant, S. et al., 2004, ApJS, 154, 118
- Smail, I., Ivison, R.J., Blain, A.W., 1997, ApJ, 490, L5
- Smail, I., Ivison, R.J., Blain, A.W., Kneib, J.-P., 2002, MNRAS, 331, 495
- Waskett, T., et al., 2003, MNRAS, 341, 1217
- Webb, T.M.A., Lilly, S. J., Clements, D.L., Eales, S., Yun, M., Brodwin, M., Dunne, L., Gear, W. K., 2003, ApJ, 597, 680
- Webb, T.M.A., et al., 2003, ApJ, 587, 41
- Webb, T.M.A., et al., 2003, ApJ, 582, 6
- Werner, M., et al., 2004, ApJS, 154, 1